

Fits perfectly into your workflow

Due to automated sample preparation, our new CLAM-2040 makes analysis easier and more efficient than ever before – perfect also for less experienced users. You save time and effort and avoid errors resulting from a manual pretreatment. In addition, you get full flexibility because the CLAM-2040 can be combined with other devices like the LCMS-9050 Q-TOF and compatible with LIS & LAS (option).

Easy to use and to maintain:
reduced workload for operators.



Operational productivity:
automates all steps from pretreatment to result.

Full flexibility:
compatible with a variety of Shimadzu devices.



RESEARCH ARTICLE

A biotechnological approach for the production of new protein bioplastics

Francesca De Marchis¹ | Tania Vanzolini² | Elisa Maricchiolo² | Michele Bellucci¹  | Michele Menotta² | Tomas Di Mambro² | Annalisa Aluigi² | Andrea Zattoni³ | Barbara Roda³ | Valentina Marassi³ | Rita Crinelli² | Andrea Pompa² 

¹Institute of Biosciences and Bioresources, Division of Perugia, National Research Council, Perugia, Italy

²Department of Biomolecular Sciences, University of Urbino Carlo Bo, Urbino (PU), Italy

³Department of Chemistry G. Ciamician, University of Bologna, Bologna (BO), Italy

Correspondence

Andrea Pompa, Department of Biomolecular Sciences, University of Urbino Carlo Bo, Via Aurelio Saffi, 2 – 61029 Urbino (PU), Italy. Email: andrea.pompa@uniurb.it

Funding information

European Union – NextGenerationEU under the Italian Ministry of University and Research (MUR) National Innovation Ecosystem, Grant/Award Number: ECS00000041 – VITALITY—CUPH33C22000430006

Abstract

The future of biomaterial production will leverage biotechnology based on the domestication of cells as biological factories. Plants, algae, and bacteria can produce low-environmental impact biopolymers. Here, two strategies were developed to produce a biopolymer derived from a bioengineered vacuolar storage protein of the common bean (phaseolin; PHSL). The cys-added PHSL* forms linear-structured biopolymers when expressed in the thylakoids of transplastomic tobacco leaves by exploiting the formation of inter-chain disulfide bridges. The same protein without signal peptide (Δ PHSL*) accumulates in *Escherichia coli* inclusion bodies as high-molar-mass species polymers that can subsequently be oxidized to form disulfide crosslinking bridges in order to increase the stiffness of the biomaterial, a valid alternative to the use of chemical crosslinkers. The *E. coli* cells produced 300 times more engineered PHSL, measured as percentage of total soluble proteins, than transplastomic tobacco plants. Moreover, the thiol groups of cysteine allow the site-specific PEGylation of Δ PHSL*, which is a desirable functionality in the design of a protein-based drug carrier. In conclusion, Δ PHSL* expressed in *E. coli* has the potential to become an innovative biopolymer.

KEYWORDS

biopolymer, disulfide bridges, *E. coli*, phaseolin, transplastomic plants

Abbreviations: AFM, atomic force microscope; DTT, dithiothreitol; FFF, field flow fractionation; FMM, force modulation microscopy; FW, fresh weight; HF5, hollow-fiber flow field-flow fractionation; HFIP, 1,1,1,3,3,3-hexafluoroisopropanol; HRP, horseradish peroxidase; IBs, inclusion bodies; IPTG, isopropylthio- β -D-galactopyranoside; MALS, multi-angle light scattering; MSH, β mercaptoethanol; PBs, protein bodies; PEG, polyethylene glycol; PHSL, phaseolin; PHSL*, phaseolin (PHSL), with single cysteine residue inserted in the C-terminal tail; Rg, radius of gyration; RT, room temperature; TSP, total soluble proteins; Δ PHSL*, phaseolin (PHSL), with single cysteine residue inserted in the C-terminal tail lacking its own signal peptide.

Francesca De Marchis and Tania Vanzolini contributed equally to this work.

This is an open access article under the terms of the Creative Commons Attribution License, which permits use, distribution and reproduction in any medium, provided the original work is properly cited.

© 2023 The Authors. *Biotechnology Journal* published by Wiley-VCH GmbH.

1 | INTRODUCTION

The impact of petroleum-based materials on the biosphere is one of the greatest problems to be faced. To this end, the study of biodegradable polymers derived from bioreactors has been constantly increasing. Unfortunately, there are few biodegradable biopolymers produced to date that show processing and mechanical properties of interest for industrial purposes. Due to their high and easy processability, high stability against mechanical and thermal stresses and low

cost, petroleum-based plastics have been widely used for a variety of applications, including biomedical uses, drug delivery^[1] systems and cosmetic personal care materials. However, it has been recognized that the widespread use of these synthetic plastics represents a huge environmental problem due to their very slow biodegradability.^[2] The strategy proposed by the research community to address the aforementioned issues concerns the replacing of petroleum-based plastics with environmentally friendly polymers such as polysaccharides, lipids, and proteins. This approach has been widely considered for the development of innovative pharmaceutical and cosmetic formulations due to their great availability, high biocompatibility and biodegradability, and great ability to be functionalized.^[3,4]

Plant polypeptides like zeins, gluten, phaseolin, and soy proteins, are at the center of extensive research, since they can be easily processed into several kinds of materials, such as micro/nanoparticles, hydrogels, films, porous sponges, and micro/nanofibers.^[5,6] However, the most well-known issues to overcome in their processing lie in their poor plasmatic half-life and poor mechanical properties, especially in physiological aqueous environments, where they tend to swell until complete dissolution.^[4] Strategies used to address these issues include protein PEGylation to increase the plasmatic half-life, or the use of cross-linking agents to increase stability and mechanical properties. It is well known that the chloroplast compartment could be used to increase production of heterologous proteins of pharmaceutical-industrial interest^[7,8] and biodegradable polymers in transgenic plants.^[8] Furthermore, the plastid compartment accomplishes some of the post-translational modifications of proteins, such as the correct formation of disulfide bonds.^[9] The formation of disulfide bridges within the chloroplast can occur both in the stroma and in the thylakoids, although it seems that the latter have a more suitable environment for carrying out this type of post-translational modification.^[10] Trying to devise a new plant protein to be used as a biodegradable biopolymer, we recently showed that a genetically modified phaseolin (PHSL), a vacuolar seed protein of *Phaseolus vulgaris*, with a single cysteine residue inserted in the C-terminal tail (PHSL*),^[11] is able to form high-molecular weight species of tens of million Da, when expressed in tobacco chloroplast.^[12] These PHSL polypeptides are linked by inter-chain disulfide bridges, confirming the positive impact of the Cys modification on polymerization.

In this study, we want to compare two different biotechnological platforms for producing a biopolymer based on PHSL* polymerization. The first platform is represented by bacteria expressing a different version of the PHSL* protein, lacking its own signal peptide (Δ PHSL*),^[13,14] which in bean seeds targets PHSL in the endoplasmic reticulum. In fact, it is known that the presence of signal sequences can lead to a decrease in the quality and accumulation of recombinant proteins when expressed in *Escherichia coli*.^[15] A second biotechnological platform consists of transplastomic tobacco plants, those previously obtained^[13] expressing PHSL* and the ones transformed here with the new plastid vector coding for Δ PHSL*. The plastidial Δ PHSL*/PHSL*-based polymeric forms were biochemically characterized and the results showed that the absence of the signal peptide dramatically decreased the translation of Δ PHSL* mRNA and the accu-

mulation of the corresponding protein. Conversely, the lack of signal peptide did not produce the same negative effects in bacteria where Δ PHSL* is expressed at higher levels than plastidial PHSL*. Moreover, Δ PHSL* in bacteria accumulated within easily purified protein bodies containing approximately 95% of the desired protein. The data reported here indicated that the bacterial self-crosslinking Δ PHSL* may represent a novel strategy for the production of biopolymers from natural proteins modified by genetic engineering.

2 | MATERIALS AND METHODS

2.1 | Gene constructs and plant transformation

The PHSL cDNA gene, coding for phaseolin, was amplified from plasmid pDHAT343F,^[16] with 5'NdeI Δ P (5'-tcactttctgcctcacatgatgctt-actccgggag-3') and 3'NotIIP* (5'-ccccctccggatcgcggcgctagtacaaat-gcaccctttcttccct-3') oligonucleotides, in order to introduce the NdeI and NotI restriction sites (in bold) at the 5' and 3' ends of the gene, respectively. Furthermore, the 3'NotIIP* primer has been designed in order to insert a cysteine residue (underlined) at the C terminus of the protein. After digestion with NdeI/NotI, the PCR product, where the 72-bp PHSL signal sequence was deleted, was cloned into pCR2.1-5'UTR,^[17] to obtain the pCR2.1-5'UTR- Δ PHSL* intermediate plasmid, in which PHSL is under the plastidial psbA promoter/5'UTR control. The psbA/5'UTR- Δ PHSL* cassette was excised from pCR2.1-5'UTR- Δ PHSL* by EcoRV/NotI digestion and subcloned into pLD-CTV,^[18] generating the pLD-CTV- Δ PHSL* vector. Homoplasmic Δ PHSL* transplastomic plants were obtained by particle bombardment, as previously described.^[13] T0 transplastomic plants were grown in axenic conditions before being transferred to the greenhouse for seed production. T0 seeds were sown on agar-solidified MS medium with spectinomycin (500 mg L⁻¹) in order to obtain T1, and then T2 Δ PHSL* transplastomic plants. Regarding the PHSL* transplastomic tobacco plants used in this study, they were obtained as described.^[12]

2.2 | Isolation and analysis of nucleic acids

To confirm and verify the homoplasmic state of PHSL* and Δ PHSL* plants, total DNA was isolated from their leaves with the GenElute™ Plant Genomic DNA Miniprep Kit (Merck KGaA, Darmstadt, Germany) and subjected to Southern blotting assay. Total DNA (2 μ g) was digested overnight with BglIII restriction enzyme and analyzed as described,^[19] using both the *trnI/trnA* tobacco region and the PHSL cDNA gene as probes. For expression analysis, total RNA was extracted from PHSL* and Δ PHSL* plants with the Nucleo Spin_RNA Plant Kit (Fisher Scientific, Loughborough, UK), and 2 μ g was electrophoretically fractionated on a 1.4% formaldehyde agarose gel. Hybridization with the cDNA PHSL probe was performed as previously described.^[19] Polysomes of PHSL* and Δ PHSL* transplastomic plants were obtained from 300 mg of leaf tissue and analyzed as previously reported.^[14] The cDNA of the PHSL gene was used as a probe.

2.3 | Protein analysis of transplastomic tobacco plants

Total proteins were extracted from leaves of transplastomic tobacco plants expressing PHSL* or ΔPHSL* homogenized with homogenization buffer (200 mM NaCl, 1 mM EDTA, 0.2% Triton X-100, 100 mM Tris-Cl, pH 7.8) supplemented with complete protease inhibitor cocktail (Roche), and analysed by SDS-PAGE and immunoblotting, as reported previously^[14] using antibodies against phaseolin (1:10000).

Pellet derived from the sucrose gradient of total proteins previously extracted^[12] from transplastomic tobacco leaves expressing PHSL* was solubilized by homogenation buffer containing SDS. The homogenate was loaded on a linear 5%–25% w/v sucrose gradient made in 150 mM NaCl, 1 mM EDTA, 0.1% Triton X-100, and 50 mM Tris-Cl, pH 7.5. After centrifugation at 141,000 × g for 24 h at 4°C in a Beckman SW28 rotor, fractions of 900 μL were collected and analyzed by SDS-PAGE and protein blotting with antiphaseolin antibodies. To analyze the presence of PHSL* dimeric forms, fractions 5 containing the putative dimers was treated with loading buffer containing 0.1 M DTT. Pulse-chase analyses were performed on protoplasts derived from young tobacco leaves of plants expressing PHSL* and ΔPHSL* as described.^[20] Briefly, protoplasts were subjected to pulse-chase labelling with Pro-Mix (a mixture of [35S]Met and [35S]Cys; GE Healthcare Little Chalfont, Buckinghamshire, United Kingdom) for 1 h and chased for indicated time, and then homogenized using a homogenization buffer (150 mM Tris-Cl, pH 7.5, 150 mM NaCl, 1.5 mM EDTA, 1.5% Triton X-100 and Complete protease inhibitor cocktail [Roche]). Total proteins were immunoselected using antiphaseolin rabbit polyclonal antibodies and analyzed by SDS-PAGE. Gels were treated with AmplifyTM fluorography reagent (GE Healthcare), dried and exposed for fluorography.

2.4 | PHSL extraction from beans

For PHSL extraction and purification, *P. vulgaris* seeds (10 g) were stripped of their tegument and placed in a grinder to obtain a flour, then resuspended in PBS (1:8 w/v, i.e., 10 g in 80 mL of PBS) stirring for 48 h at 4°C, as described.^[12] Briefly, after filtering through gauze pads and centrifuge at 10,000 × g for 30 min, pH was adjusted to 4.5 by slowly adding 1 M acetic acid to induce protein precipitation. The solution was stirred for 30 min at 4°C and then centrifuged at 10,000 × g for 30 min. Pellet was collected and resuspended in PBS adjusting to neutral pH with NaOH 1N. Six hundred microliters of the prepared sample were loaded on the top of a linear 5% to 25% sucrose velocity gradient made in 150 mM NaCl, 1 mM EDTA, 0.1% Triton X-100, and 50 mM Tris-Cl, pH 7.5, and centrifuged at 141,000 × g for 24 h at 4°C in a Beckman SW28 rotor. After centrifugation, the gradient was fractionated and three aliquots of the fractions with the major PHSL content were mixed together and subjected to dialysis for 3 days, during which distilled water was replaced every 12 h, and finally freeze-dried.

2.5 | PHSL* purification from tobacco leaves

Leaves from transplastomic tobacco plants, were grinded cold in a mortar with a homogenization buffer (200 mM NaCl, 1 mM EDTA, 100 mM Tris-Cl, pH 7.8) without detergents. The homogenate was filtered with a gauze to eliminate the debris, subsequently was centrifuged at 2500 × g for 5 min at 4°C to recover the chloroplasts and eliminate most of leaf proteins. The recovered chloroplasts were then solubilized with the same buffer added with 2% of Triton X-100, which solubilizes the plastidial proteins and then loaded on a linear 5%–25% w/v sucrose gradient made in 150 mM NaCl, 1 mM EDTA, 0.1% Triton X-100, 50 mM Tris-Cl, pH 7.5. After centrifugation at 39,000 × g, for 8 h at 4°C in a Beckman SW40 rotor, the supernatant was discarded and the pellet containing PHSL* aggregates was recovered by a minimal amount of distilled water (1 mL). The resulting PHSL* aggregates were subjected to dialysis overnight to eliminate sugar and other contaminants. The purified sample was used for HF5-UV-FLD-MALS analysis, or lyophilized and analyzed under an optical or electron microscope. The scheme of PHSL* purification is reported in Figure S4.

2.6 | Phaseolin expression in *E. coli*

ΔPHSL and ΔPHSL* coding sequences were cloned between PmlI and HindIII sites of the pET-45b(+) vector by GenScript®. This vector allows expression of the proteins with a 6His tag at the N-terminus. Sequences were optimized for bacterial expression. Plasmids were transformed into competent BL21(DE3) *E. coli* cells. Bacteria were grown at 37°C in Luria Bertani (LB) medium (tryptone 10 g L⁻¹, yeast extract 5 g L⁻¹, NaCl 10 g L⁻¹, pH 7.5) supplemented with ampicillin 100 μg mL⁻¹ (A100). Protein expression was induced when the culture reached an OD_{600nm} of 1.0 by adding 0.4 mM isopropylthio-β-D-galactopyranoside (IPTG) (Sigma-Aldrich). Bacterial pellets were resuspended in lysis buffer (Na/K phosphate buffer 50 mM, Triton X-100 0.5% v/v, pH 7.4), sonicated three times on ice (Ultrasonic Cell Crusher 60 W, 30 s and 1 min pause) and centrifuged at 4°C for 20 min at 14,000 × g. Soluble fractions were transferred into fresh tubes and pellets were solubilized in Na/K phosphate buffer (50 mM, urea 8 M, pH 7.4) when used for analytical purposes.

To perform experiments on recombinant PHSL expression between plants and bacteria, the bacterial pellet was resuspended in Na/K phosphate buffer 50 mM, urea 8 M, pH 7.4. The suspension was sonicated once (Ultrasonic Cell Crusher 60 W, 30 s) and left rotating 1 h at RT. Then, the sample was centrifuged for 20 min at 14,000 × g at RT and the supernatant transferred into fresh tubes. For bulk production of ΔPHSL*, the bacterial pellets were disrupted by three repeated passages through the French pressure cell (Avastin, Emulsiflex B15, 10000–13000 Psi) and sonicated three times on ice (Ultrasonic Cell Crusher 120 W, 1 min and 1 min pause). After centrifugation, the insoluble fraction containing the recombinant protein was washed in lysis buffer, then in Na/K phosphate buffer (50 mM, pH 7.4) and finally in MΩ water. The resulting pellet was stored at –80°C and then

freeze-dried (Edwards freeze-dryer equipped with a vacuum pump Modulyo EF4).

2.7 | Analysis of bacteria-produced recombinant PHSL

The presence, identity and integrity of the Δ PHSL and Δ PHSL* proteins were assessed by SDS-PAGE and western immunoblotting. Samples were separated on 10% w/v polyacrylamide gels. Proteins were visualized by gel staining with Coomassie brilliant blue R-250 or electroblotted onto nitrocellulose membranes and stained with anti-6 × His tag polyclonal antibody (OriGene). Horseradish peroxidase (HRP) conjugated secondary antibody (BioRad) in combination with the enhanced chemiluminescence detection kit WesternBright ECL (Advansta) were used for detection. Images were acquired with a ChemiDoc MP Imaging System (BioRad).

2.8 | Bacterial phaseolin PEGylation

For phaseolin PEGylation, the insoluble fraction of the cell lysate was directly suspended in 100 μ L of Tris-HCl 0.1 M pH 6.8, urea 8 M, EDTA 1 mM, supplemented with 5 kDa maleimide PEG (PEGmal₅₀₀₀, Sigma), a cysteine-reactive PEG reagent. The samples were incubated for 2 h at RT in the dark and the reaction was stopped by adding 0.1 M dithiothreitol (DTT). The PEGylation was confirmed by SDS-PAGE and western immunoblotting.

2.9 | Preparation of the films by casting

The freeze-dried powders of *E. coli* Δ PHSL and Δ PHSL* were dissolved in 1,1,1,3,3,3-hexafluoroisopropanol (HFIP) at a concentration of 7% w/v. The dissolution was performed under magnetic stirring overnight. After that, the solution was cast in a mold and the solvent was allowed to evaporate overnight in order to obtain the films.

2.10 | Atomic force microscopic analysis of biopolymers derived from bacteria

The XE-100 atomic force microscope (AFM; PARK Systems Inc.) was used in this study. The instrument was equipped with a 50- μ m scanner in the XY plane and a 12.5- μ m scanner in the Z direction, all controlled by the XEP 1.8.1 software. Scanners operated in a closed-loop manner and high voltage mode. The Z scanner resolution was set to 1.8 Å. The nanomechanical proprieties of the surfaces were acquired by setting the AFM in force modulation microscopy (FMM). For this purpose, a 36A cantilever (Micromasch) with 1 N m⁻¹ typical force constant and a resonant frequency of 192 KHz was employed. Cantilever free amplitude was calibrated as described by PARK System. Topography, FMM

amplitude, FMM phase signal, and cantilever deflection were simultaneously acquired during 20 × 20 μ m imaging at 0.2 Hz. The scanned area was randomly chosen for each film. AFM images were analyzed by XEI software.

2.11 | HF5-UV-FLD-MALS analyses

Size separation and molar mass determination of putative biopolymers by HF5-UV-FLD-MALS were performed essentially as described.^[12] The conventional HF5 method is composed of four steps: focus, focus-injection, elution, and elution-injection. During the focus step, the mobile phase is split into two different streams entering from the inlet and outlet; and during focus-injection, the flow settings remain unvaried and the sample is introduced into the channel through the inlet to be focused on a narrow band. In this step, particles smaller than the cutoff are filtered away from the sample.^[21] In the elution step, the mobile phase enters the channel inlet and splits into a radial component out of the fiber's pores (cross-flow, Vx), and a longitudinal component that reaches the detectors (channel flow, Vc); lastly, during elution-injection, the flow is redirected into the injection, allowing for any remaining sample inside the channel and the system to be released. Due to the parabolic flow profile of the carrier flow, smaller particles experience higher average flow velocities than larger ones. In this normal elution mode, the analyte retention time is a function of its apparent diffusion coefficient. Hence, the analyte retention volume can be related to its diffusion coefficient, and consequently, to its hydrodynamic size using Stoke's equation and a calibration can be performed. Multi-angle light scattering (MALS) was used to measure the molar mass of eluted proteins. It allows for the absolute determination of particle radius of gyration (Rg), and, given the dn/dc and absorptivity values of the analyzed species, the molar mass value of the eluted species.^[22]

To characterize PHSL* plant extract, 30 μ L of a 0.3 mg mL⁻¹ suspension were injected, while for the *E. coli* extract 1 mL of water was added to 0.1 mg of lyophilized Δ PHSL* protein and the resulting mix was sonicated for three cycles of 5 min. Then, the supernatant was transferred in a vial for injection in FFF.

3 | RESULTS

Homoplasmic T2 transplastomic plants expressing Δ PHSL* were obtained in this study using a biolistic transformation protocol.^[13] These plants have the Δ PHSL* gene inserted into the plastome, coding for a modified phaseolin without the signal peptide and contained a cysteine residue just before the vacuolar sorting signal sequence.^[23] Our hypothesis is that the absence/presence of the signal peptide may play a key role in the accumulation of Δ PHSL*/PHSL* in tobacco chloroplasts. Therefore, Δ PHSL* transplastomic plants were characterized and compared with the PHSL* transplastomic plants previously obtained.^[12]

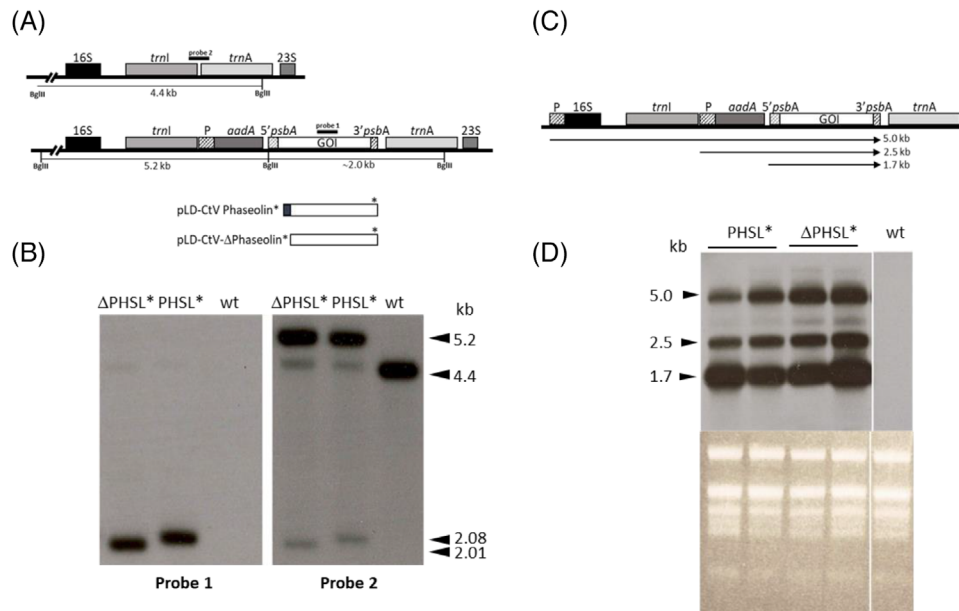


FIGURE 1 Northern and Southern blot analyses of tobacco transplastomic plants. (A) Schematic representation of the 16S/*trnI*/*trnA*/23S region of the tobacco chloroplast genome and of the plastid transformation vectors, the probes used for Southern blot analysis are indicated as probe1 (*phaseolin* gene) and probe2 (*trnI*/*trnA* region). The predicted hybridizing fragments, after digestion with *Bgl*III restriction enzyme and Southern blot analysis, are indicated in kb. (B) Southern blot analysis of PHSL* and ΔPHSL* transformants with probe1, *phaseolin* gene (left panel), and probe 2, *trnI*/*trnA* region (right panel), showing transgenes plastome integration. The probe 1 produced two slightly different fragments due to the absence of the DNA sequence coding for the signal peptide in the ΔPHSL* plant. The faint fragments around 4.5 kb in the transplastomic plants are likely promiscuous plastid DNA already present in the nucleus, as already reported.^[13] (C) Scheme of the transcription pattern expected for the transplastomic PHSL* and ΔPHSL* genes (GOI). Horizontal arrows represent expected transcripts and their sizes. (D) Northern blot analysis on total RNA extracted from PHSL*, ΔPHSL*, and wild type (wt) plants. As a loading control, rRNA stained by ethidium bromide is shown in the lower panel. The wt sample is shown separately but belongs to the same agarose gel, which contained other four RNA samples close to the wt lane that have been not shown because not inherent to this study. Phaseolin gene was used as a probe. Numbers indicate molecular mass markers in kb. P, Prn promoter; aadA, aminoglycoside 3'-adenylyl transferase gene; 5'psbA, psbA promoter/5'UTR; 3'psbA, psbA terminator; GOI, gene of interest.

3.1 | Generation of transplastomic tobacco plants expressing ΔPHSL* protein

ΔPHSL* gene was cloned in a plastid expression cassette based on the same vector, pLD-CtV, already used to clone the PHSL* gene (Figure 1A). These vectors targeted the transgene cassette to the 16S-*trnI*/*trnA*-23S region of the chloroplast genome. After particle bombardment of tobacco leaves with the pLD-CtV-ΔPHSL* plasmid and two rounds of regeneration on spectinomycin-containing medium, several T0 transplastomic lines were obtained which were self-fertilized to the T2 progeny. To screen for transgene integration in the plastid DNA and investigate the integrity of the transgene cassette, ΔPHSL* transplastomic lines were analyzed by Southern blot to determine whether they were homoplasmic. The Southern analyses included also the PHSL* transplastomic plants, but these experiments, as all the further analyses in the text on the PHSL* transformants, were new because they were produced only for this study. Total leaf DNA was cut with *Bgl*III and probed with a *phaseolin* or a *trnI*/*trnA* probe, producing the expected fragments for transplastomic DNA (Figure 1B). The *phaseolin* probe produced only a fragment of around 2.0 kb, while the *trnI*/*trnA* probe identified both the 2.0 kb and the 5.2 kb fragment in the transplastomic plants, and the WT 4.4 kb fragment. The homoplasmic

state of the T0 transplastomic plants was demonstrated with a seed germination test on selective antibiotic, showing that all the progenies of these plants were resistant to spectinomycin, as expected for a maternally inherited plastid gene (Figure S1). Northern blotting analyses were carried out in order to verify the correct transcription pattern expected for the transplastomic PHSL* and ΔPHSL* genes (Figure 1C,D). Taken together, these analyses indicate that the insertion of the two exogenous genes within the tobacco plastome occurred correctly.

3.2 | Targeting to the thylakoid compartment increases the accumulation of PHSL* protein in transplastomic tobacco plants

The intraplastidial localization of heterologous proteins expressed in the tobacco chloroplast appears to have an important effect on their accumulation in the chloroplast. Therefore, we compared the level of accumulation of PHSL* with that of ΔPHSL*, which should have a different localization due to the absence of its own signal peptide.^[13]

Total proteins extracted from T2 transplastomic plants expressing the two versions of mutated phaseolins were analyzed using SDS-PAGE and western blot with anti-PHSL antibodies. The signal intensity

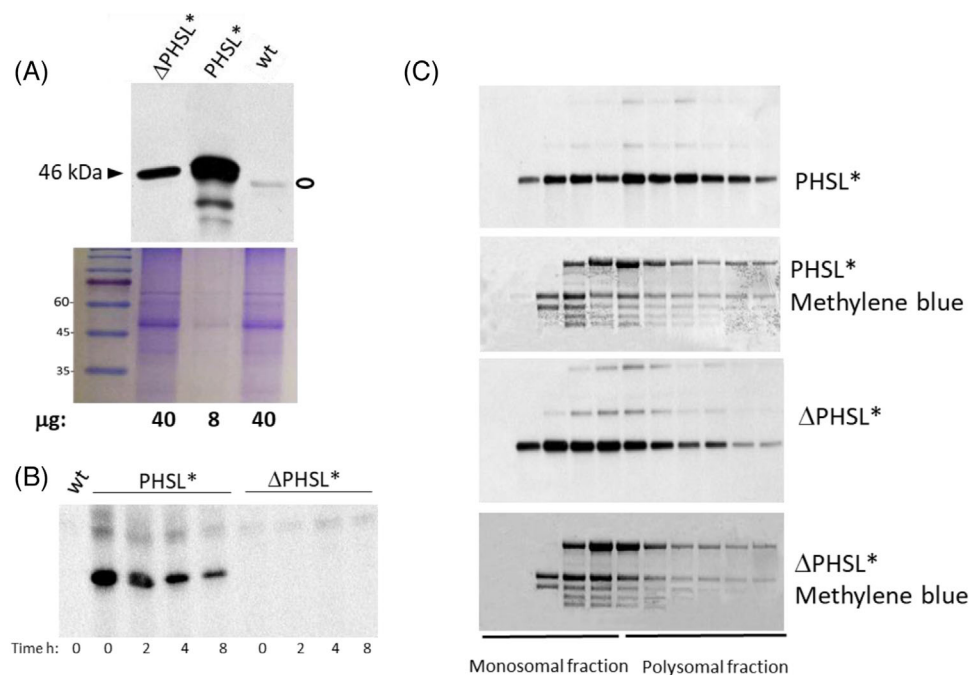


FIGURE 2 PHSL* and Δ PHSL* accumulation in tobacco chloroplasts. (A) Total proteins extracted from leaves of a WT plant or transplastomic plants expressing PHSL* or Δ PHSL* were separated by SDS PAGE and immunoblotted with antiphaseolin antiserum. The black arrowhead indicates the phaseolin polypeptide. Empty ellipse: contaminant peptide. Numbers on bottom indicate the amount of total proteins loaded in the gel, protein stained by Coomassie is shown as a loading control. (B) Protoplasts of transplastomic tobacco plants were pulse labeled for 1 h and tracked for the indicated times. The homogenized cells were immunoprecipitated with antiphaseolin antiserum and analyzed by SDS-PAGE and fluorography. (C) Polysome analysis was performed from PHSL* or Δ PHSL* plant leaves through a 15%–55% sucrose gradient fractionation. An equal proportion of RNA isolated from each fraction was analyzed by Northern blot using a phaseolin probe. The ribosomal RNA fractionation profile is visualized by methylene blue staining. Lanes 1–5 and lanes 6–1 represent monosomal and polysomal fractions, respectively.^[14]

of the 46-kDa bands was quantified by densitometric analysis (data not shown), indicating that PHSL* accumulated almost 50 times more than Δ PHSL* (Figure 2A). To verify the mechanism that leads to this discrepancy in accumulation rate, pulse-chase experiments were carried out that investigated both the correct synthesis of the exogenous protein and the translation of the foreign gene. Our experimental analyses showed that, while the PHSL* protein was detected at the first chase point and showed a half-life of approximately 4–6 h, the Δ PHSL* protein was undetectable, probably because it was present at levels below the experiment detection limit (Figure 2B). The presence of comparable recombinant mRNA levels between PHSL* and Δ PHSL* plants (Figure 1D) suggests that the lack of accumulation of the Δ PHSL* protein is due to changes in the translation of the mRNA. Thus, polysome analysis was performed in homogenates of transplastomic PHSL* and Δ PHSL* leaves by fractionation on a sucrose gradient, followed by northern blotting experiments with a probe that binds to *phaseolin* mRNA. Our data reveal that, while PHSL* mRNA was predominantly associated with actively translating polysomes, mRNA from Δ PHSL* samples was poorly translated, as the mRNA was largely detected in the first fractions of the gradient (Figure 2C). Our experiment indicates a significant reduction in the mRNA translation activity of Δ PHSL* mRNA compared to PHSL* mRNA, confirming the existence of a self-regulating mechanism that manages the translation of exogenous mRNAs in the tobacco chloroplast.^[14] To confirm this hypothesis,

localization experiments were performed on soluble and membrane fractions of chloroplasts expressing PHSL* and Δ PHSL* separated using SDS-PAGE and analyzed by western blot with anti-phaseolin antibodies (Figure S2A). Our analyses indicate that both recombinant proteins are detected in the membrane fractions containing thylakoid structures. However, experiments to detach the proteins associated with the membranes by treating the thylakoids with salt (NaCl) or reducing agents (DTT) show that, while PHSL* is integrated into the membrane fraction, Δ PHSL* is only associated with membranes and is effectively removed by both the salt and even more so by the DTT treatment (Figure S2B). We can therefore conclude that a self-regulating mechanism senses the presence of Δ PHSL* protein because it is only associated with thylakoid membranes, whereas PHSL* escapes from this regulatory mechanism due to its integration into the membrane fraction (this study and ref.[14]).

3.3 | The plastid environment allows the formation of PHSL* disulfide bonds

Our aim was to produce a protein-based biopolymer and therefore, from here on out, we focused our studies on the transplastomic plants expressing PHSL*, the protein with the highest accumulation rate. The cysteine residue in the C-terminal region of PHSL* was able to

trigger the formation of dimers when the protein is expressed at the nuclear level, but not more complex aggregation structures.^[11] These dimers are not present in bean seeds, where PHSL is a homotrimeric glyco-protein, with the three similar polypeptides linked mainly by hydrophobic interactions. Recently, it has been shown that the internal environment of genetically modified tobacco chloroplasts is able to support the formation of supramolecular complexes of PHSL* linked together by inter-chain disulfide bridges.^[12]

Here, in order to further investigate the role of the inter-chain disulfide bonds on the aggregation of PHSL* expressed in the chloroplast, the purified supramolecular complexes were homogenated with SDS, which was capable of breaking down PHSL* trimers, but not the covalently-bonded disulfide bridges. The homogenate was analyzed using a velocity sucrose gradient in order to demonstrate the presence of both the PHSL* monomer (46 kDa) and dimers (90 kDa, Figure S3A top). The molecular weights of the two forms are confirmed by the shift of the 90 kDa peak from the 4th to the 5th fraction (Figure S3A bottom). To confirm the presence of disulfide bridges, fraction 5 of the gradient was treated with a strong reducing agent (DTT). The DTT-treated sample was compared with the untreated sample in western blotting experiments. This experiment shows the disappearance of the 90 kDa band in the presence of the reducing agent (DTT), confirming the formation of inter-chain disulfide bridges due to cysteine insertion in the C-terminal tail of the protein (Figure S3B).

We then wanted to verify the physical-mechanical structure of the PHSL* supramolecular complexes produced in the chloroplasts of tobacco leaves. The homogenate obtained from the chloroplasts was separated by ultracentrifugation, and the fraction that reaches the bottom of the sucrose gradient containing the PHSL* aggregates was recovered (Figure S4). This material was lyophilized and subjected to macro and microscopic analysis (Figure S5). The images obtained by optical and scanning electron microscope indicated that the structure in which these aggregates are organized was ordered both at macroscopic and microscopic level (Figure S5A and S5B).

3.4 | Δ PHSL and Δ PHSL* were expressed at a high level in *E. coli* cells and accumulated in inclusion bodies

After having exploited plant cells as an expression system, we next sought to evaluate the expression of mutated PHSL in bacterial cells in order to compare the two biotechnological platforms. Considering that in *E. coli* the signal peptide could negatively influence the folding of the protein itself,^[24] we designed two constructs encoding for Δ PHSL* and its related control without cys, Δ PHSL. Both constructs were cloned into the pET45b(+) expression vector, which was then transformed in *E. coli* BL21(DE3) cells. These cells were grown at 37°C and expression of the recombinant proteins was induced using IPTG. SDS-PAGE analysis of the soluble and insoluble fractions derived from the lysates obtained from cells induced for different times, showed the appearance of a protein band with a molecular weight consistent with that of Δ PHSL* and Δ PHSL (about 46 kDa) (Figure 3A). The band was undetectable in non-

induced cells (lanes 1 and 6 for Δ PHSL and 10 and 15 for Δ PHSL*). Both recombinant proteins accumulated in the insoluble fraction as inclusion bodies (IBs), where they represented the most abundant protein species (lanes 7–9 and 16–18). The highest level of protein expression was obtained at 2 h post induction (lanes 8 and 17) (Figure 3A). Identity and integrity of the proteins was assessed by immunoblotting analysis using an antibody against the His tag, which selectively stained the 46 kDa protein band observed in the insoluble fraction; only a very faint signal was detected in the soluble fraction, confirming successful expression of Δ PHSL*/ Δ PHSL as IBs (Figure 3B).

3.5 | PEGylation and crosslinking of Δ PHSL* in *E. coli*

Based on the above results, bulk protein production for biomaterial preparation involved harvesting the cells at 2 h post induction, complete cell lysis using a French pressure cell, sonication, separation of IBs by centrifugation, and extensive washing of IBs to remove contaminant proteins. The final material was lyophilized, and an aliquot was analysed by SDS-PAGE under reducing and non-reducing conditions. As shown in Figure 4A, both proteins migrated at the expected molecular weight as a single band. Under non-reducing conditions, the electrophoretic mobility of Δ PHSL did not change, while a partial up-shift of the band was observed for Δ PHSL*, demonstrating that it is partially oxidized by forming disulfide-bonded higher molecular weight adducts through its cys residue. To assess whether Δ PHSL* partial oxidation occurred inside cells or during IBs processing, the redox state of the cys thiol group of Δ PHSL* was evaluated by solubilizing IBs in UREA buffer containing maleimide PEG, a cysteine-reactive PEG reagent. It is known that mal-PEG alkylation of sulfhydryl results in an apparent molecular mass shift when observed by SDS-PAGE. Consistently, SDS-PAGE analysis of PEGylated proteins resulted in an up-shift of the protein band only in the case of Δ PHSL* (Figure 4B), while no differences were observed for Δ PHSL, which does not contain cys residues, demonstrating specificity of the PEGylation reaction. This evidence highlights that Δ PHSL* is not oxidized within bacterial cells, as expected due to the highly reducing environment of *E. coli*. Therefore, Δ PHSL* probably accumulates in IBs in a reduced form and the oxidation process begins when the protein comes into contact with atmospheric oxygen during the purification process, resulting in partial oxidation as observed in Figure 4A.

In order to study the filmation process, both Δ PHSL and Δ PHSL* extracted from bacteria were dissolved into HFIP at the same concentration of 7% w/v. Polymeric films were obtained by casting, and letting the solvent evaporate. As shown in Figure 5, smooth and transparent films were obtained with both proteins. In order to observe the differences at nano-mechanical level due to the presence of cysteine in Δ PHSL*, an atomic force microscope was used, which receives impulses from a punch that scans the surface of the two films. The mean cantilever amplitude collected in force modulation microscopy analyses (FMM) is sensitive to the local nanomechanical stiffness of the

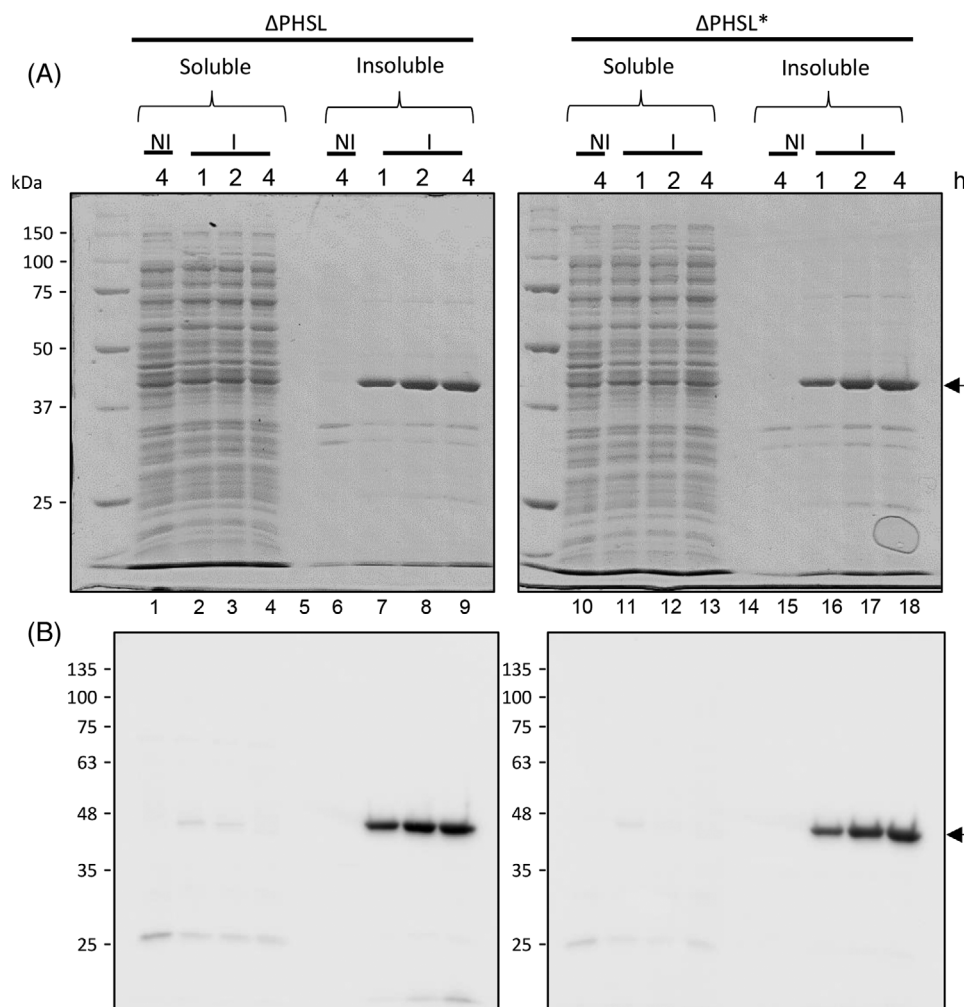


FIGURE 3 Expression of Δ PHSL and Δ PHSL* phaseolin in *E. coli*. (A) SDS-PAGE and (B) western immunoblotting analyses of the soluble (lanes 1–4 and 10–13) and insoluble (lanes 6–9 and 15–18) fractions obtained from lysates deriving from non-induced (lanes 1, 6, 10, 15) and induced (lanes 2–4, 7–9, 11–13, 16–18) bacterial cells for different times (h). Ten micrograms of soluble proteins and an equal volume of insoluble proteins were loaded on a 10% v/v polyacrylamide gel. The gels were stained with Coomassie brilliant blue (A) or electroblotted and stained with an anti-His antibody (B). Molecular weight markers are shown on the left. Arrows at the right indicate the corresponding recombinant phaseolin protein.

sample; in particular, it increases with increasing sample stiffness. The Δ PHSL surface showed prevalent green-blue regions, indicating cantilever amplitudes between 3.00 and 3.60 nm (Figure 5). On the other hand, the Δ PHSL* surface showed widely diffused green-yellow-red regions, indicating cantilever amplitudes between 7.00 and 10.00 nm. The mean cantilever amplitude of the Δ PHSL* film was about two-fold higher than that of the Δ PHSL film, indicating a significantly higher nanomechanical stiffness of Δ PHSL* compared to the control. This could be attributed to the formation of disulfide crosslinking bridges between the thiol groups of the cys residues present only in Δ PHSL*, which occurred during HFIP evaporation by atmospheric oxidation. An increased stiffness of a biomaterial induced by crosslinking is a very common behavior that has also been observed by several authors for hydrogels present in the extracellular matrix,^[25] as well as for polyelectrolyte multilayer films.^[26] Based on these results, we focused our next experiments on Δ PHSL*-expressing *E. coli*.

3.6 | Comparative analysis between the two bioreactors for the production of engineered phaseolin

In order to verify the aggregation states of engineered PHSL extracted from plants or bacteria, we analyzed the protein fraction containing PHSL* purified from transplastomic plants as described in Figure S4 and the protein fraction containing Δ PHSL* purified from *E. coli* as described in Figure S6. The analysis was performed via hollow-fiber flow field-flow fractionation (HF5) coupled to UV, fluorescence and multi-angle laser scattering detection. HF5 allows for the selective size-based separation of nano- and micro-sized particles, while smaller species are filtered out in the pre-separation step (see Section 2). Online detectors allow the evaluation of protein content and calculate the molar mass values for the eluted species. Moreover, through FFF theory it is possible to calibrate the method to predict

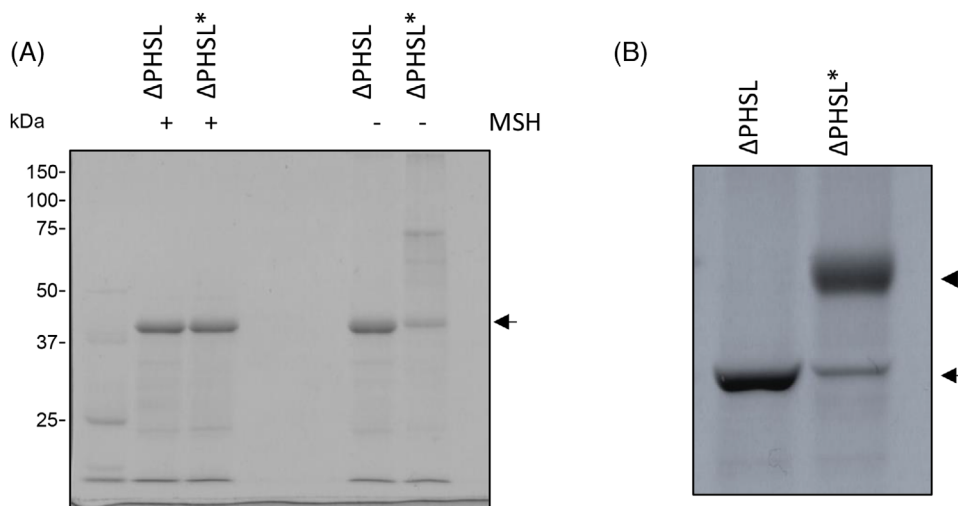


FIGURE 4 SDS PAGE analysis of Δ PHSL* cysteine oxidation and pegylation. (A) SDS-PAGE of Δ PHSL and Δ PHSL* under reducing and non-reducing conditions. Five micrograms of purified proteins were diluted in sample buffer supplemented or not with β mercaptoethanol (MSH) separated on 10% v/v polyacrylamide gel and stained with Coomassie brilliant blue. (B) SDS-PAGE of recombinant phaseolin after PEGylation with mPEG 5000. Ten micrograms of proteins were loaded on 8% v/v polyacrylamide gel and stained with Coomassie. Arrows at right indicate the corresponding recombinant phaseolin. Arrowhead indicates PEGylated Δ PHSL*.

the retention time according to hydrodynamic size. In Figure 6, the fluorescence signal (tuned to protein intrinsic fluorescence) was overlaid with the molar mass calculated by multi-angle light scattering. The method size calibration was also reported (top), and the dependabil-

ity of the model was confirmed by the retention times of standard injections of proteins (albumin, immunoglobulin, shown as dashed line in Figure 6B) congruent with the predicted ones. The analysis of the plant PHSL* protein fraction showed no evidence of protein species

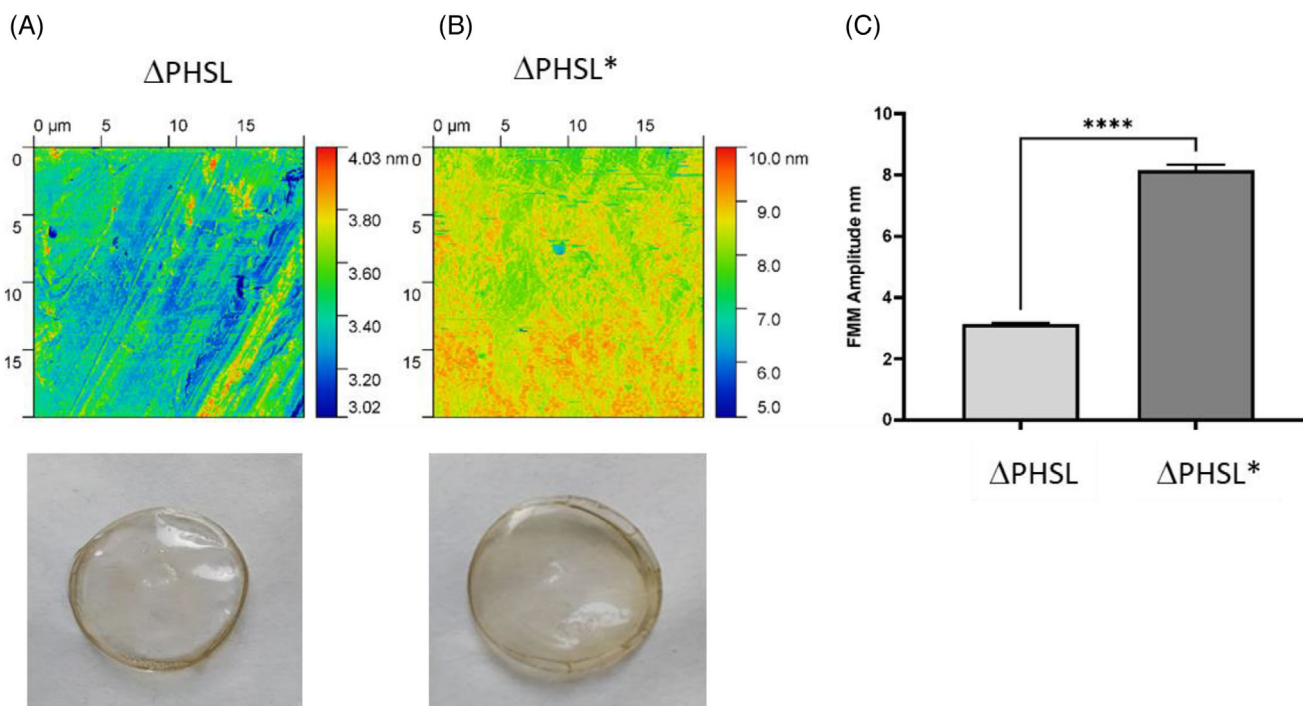


FIGURE 5 Comparison of the mechanical properties of Δ PHSL (A) and Δ PHSL* (B) expressed in *E. coli*. Representative images of FMM amplitude signal, expressed as nm in the bar graph, of the analyzed samples (above) and films obtained by casting and letting HFIP evaporate (below). FMM signals from all image pixels were collected and plotted as a graph (C). Amplitude signal of Δ PHSL* resulted higher than that of the Δ PHSL sample (Welch's test $p < 0.0001$) indicating an increase of surface stiffness.

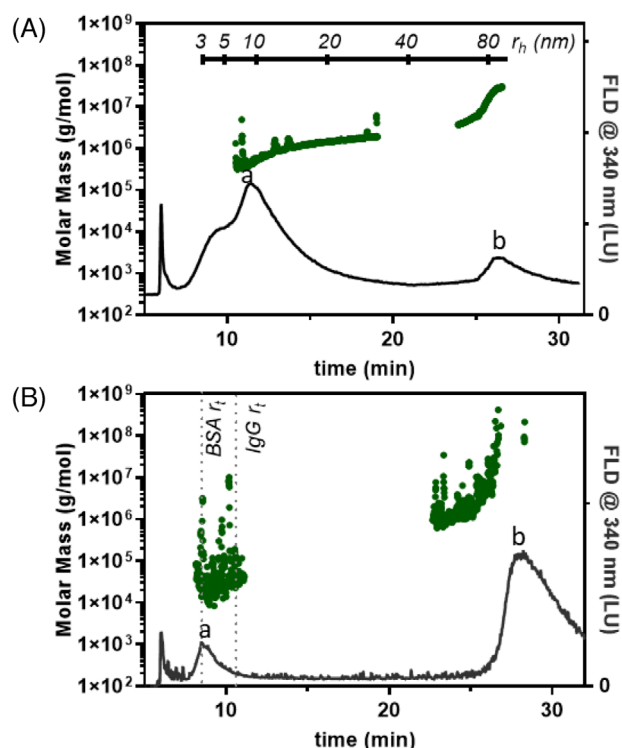


FIGURE 6 Separation and mass characterization of PHSL* choroplast extracts (A) or Δ PHSL*-expressing *E. coli* extracts (B) by hollow fiber flow field flow fractionation with multi angle light scattering, fluorescence and UV detection (HF 5 MALS UV FLD). (A) Thylakoid extract. Average molar mass (Da) of the two eluted populations: a, 1.17×10^6 ($\pm 12\%$); b, 1.71×10^7 ($\pm 10\%$). Black line (top): size calibration of the devised method as from FFF theory. (B) *E. coli* extract. Average molar mass (Da) of the two eluted populations: a, 6.8×10^5 ($\pm 15\%$); b, 2.3×10^7 ($\pm 18\%$). Dashed lines: experimental retention time values of standard albumin (BSA) and Immunoglobulin G (IgG) injections to verify the reliability of FFF method calibration. Black line: fluorescence signal ($\lambda_{\text{ex}} = 280 \text{ nm}$, $\lambda_{\text{em}} = 340 \text{ nm}$). Green dots: molar mass values calculated from MALS and UV signals.

corresponding to PHSL* trimers and oligomers, which should be eluted at earlier retention times, while two protein populations are detected and separated (Figure 6A). The first, peaking at 11 min and consisting of the majority (86%) of the sample, had an average molar mass of 1.2 MDa, while the second eluted at the field release, reached tens of millions of Da. The presence of these high-molar-mass species, together with the lack of PHSL* oligomers, suggested the successful formation of PHSL* polymers. The Δ PHSL* protein fraction from *E. coli* proved to be only partially soluble in water and PBS, suggesting that Δ PHSL* was present at a highly polymerized state. The soluble fraction was injected in FFF and showed to contain a small amount of a first aggregate population (averaging 700 kDa), while the majority of the sample was totally retained, and had a mass distribution reaching 10 MDa (Figure 6B).

To quantify the phaseolin polymers, semi-quantitative western blots using anti-PHSL antibodies were attempted (Figure 7). Western analysis was carried out in triplicate using *E. coli*/plant total soluble proteins, and purified PHSL as a standard, loaded in different amounts. To avoid saturated band signals, the amount of *E. coli* total proteins loaded on

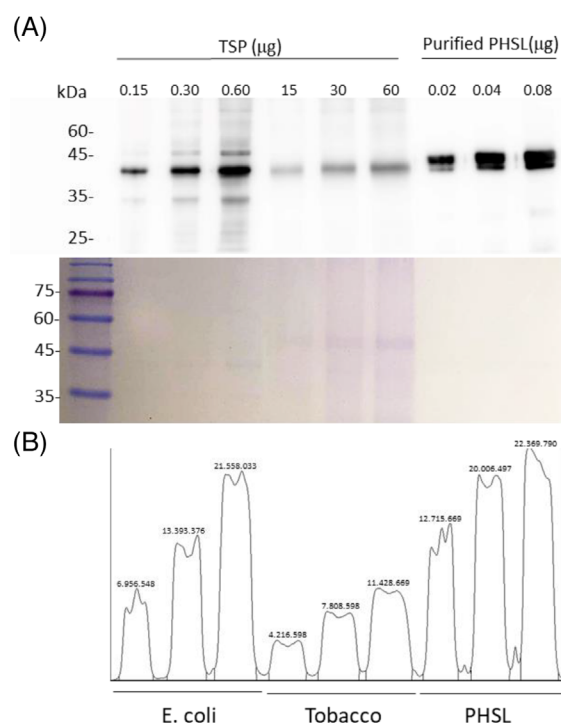


FIGURE 7 Comparison of engineered phaseolin accumulation in transplastomic tobacco and *E. coli*. (A) Total soluble proteins (TSP) extracted from leaves of PHSL* transplastomic plants or from transformed *E. coli* cells expressing Δ PHSL*, were separated by SDS PAGE and immunoblotted with antiphaseolin antiserum. This blot is an example of the three blots performed. Numbers on top indicate the amount of total proteins loaded in the gel and the amount of purified PHSL. Protein stained by Coomassie is shown as a loading control. (B) The peaks indicate in arbitrary units the measurement of the phaseolin specific bands in (A) by densitometric analysis (Image-J2 image processing software, version 2.9.0/1.53t). Numbers at the left indicate molecular mass in kDa.

the gel was 100 times lower in comparison to the tobacco extracts. The amount of PHSL* polymers in tobacco leaves was first expressed as a percentage of total soluble proteins (TSP) and was roughly 0.03% of TSP, whereas the bacterial Δ PHSL* was expressed at 6.7% of TSP. There was a 300-fold increase of mutated PHSL polymers in bacterial TSP compared to the plant TSP. As it is not easy to compare the two biotechnological platforms (plants in greenhouse and bacterial liquid culture) for recombinant protein production, we also determined that in tobacco plants PHSL* yield was $10 \mu\text{g g}^{-1}$ fresh weight (FW), while *E. coli* cells had a Δ PHSL* yield of $1000 \mu\text{g L}^{-1}$.

4 | DISCUSSION

Proteins of high molecular weight (>25 kDa) are natural heteropolymers, thereby being ideal raw materials for the production of biodegradable plastics alternative to petroleum-derived ones. From the technological point of view, some drawbacks which limit the use of proteins as biodegradable plastics lie in their fragility, low

processability, and low mechanical properties.^[27] The blending with other polymers with suitable mechanical properties and/or the use of crosslinking agents are the most common strategies to overcome the aforementioned drawbacks. The aim of this study was to explore a new way to engineer proteins with functionalities targeted to obtain desirable chemical, processing and mechanical properties, so that they can be potential biodegradable alternatives to petroleum-derived polymers. To this end, a genetic modification of the bean storage protein PSHL has been deeply investigated. This protein has been previously modified incorporating a cysteine residue into its C-terminal amino acid chain (PSHL*) and expressing it in the plant plastids.^[12] Here, we compared two bioplatforms to produce PSHL* (or its version devoid of the signal peptide, ΔPSHL*), showing that in both plant and bacterial bioreactors engineered PSHL was present as high-molar-mass species polymers. However, if we consider the percentage of TSP, the *E. coli* cells produced 300 times more recombinant PSHL than transplastomic tobacco plants (Figure S7).

Concerning the tobacco plants, an accurate analysis of the intraplasmid localization and accumulation of PSHL* and ΔPSHL* was performed. Using different molecular biology approaches, it has been shown that the accumulation of PSHL* increased almost 50-fold if the protein was inserted into the membranes of tobacco thylakoids instead that only associated with those membranes (ΔPSHL*). Moreover, it has been shown that the chloroplast environment has the chemical-physical and potential redox characteristics to form the PSHL* disulfide bridges, inducing the accumulation of megadalton-scale biopolymeric PSHL* forms. This potentially is an excellent result, mainly because this approach could be used in plants of agricultural interest where chloroplast transformation is available, such as tomato^[28] that produce a lot of leaf biomass as waste. The insertion of the PSHL* gene at the level of the chloroplast in these species could increase the economic value of this biomass, from which it would be possible to purify a protein biopolymer usable at a pharmaceutical or industrial level. Unfortunately, the level of expression in PSHL*-expressing transplastomic tobacco plants is very low (0.03% of TSP) in comparison to the accumulation levels reported for other recombinant proteins with the transgenes localized in the plastid genome, that in some cases reached more than 50% of the leaf TSP.^[29]

Therefore, we developed an alternative strategy that involves the use of bacterial organisms as bioreactors. Often, heterologous proteins expressed in bacteria (e.g., *E. coli*) are accumulated in PBs, and for this reason, are easy to extract and purify. In this study, we show that *E. coli* expressing ΔPSHL* accumulate this protein in IBs that can be purified by simple centrifugation. ΔPSHL* is present in a reduced form in IBs and is then partially oxidized by atmosphere during the purification process, resulting in a highly polymerized state up to 10 MDa. The presence of cys residues in ΔPSHL* is a functionality that can be exploited in the design of drug delivery systems and/or scaffolds for tissue regeneration. As demonstrated, the thiol groups of cysteine allow the site-specific PEGylation of ΔPSHL*, being a desirable functionality in the design of a protein-based drug carrier. Indeed, the site-specific protein PEGylation, often carried out to increase the protein half-life in blood streamlines, improves the production/purification

processes and contributes to retain the pharmacokinetic benefits that accompany PEG attachment.^[30] Moreover, the nanomechanical stiffness of ΔPSHL* revealed that the thiol groups can be also exploited for the protein crosslinking via disulfide covalent bonds. This functionality represents a valid alternative to the use of chemical crosslinkers as glutaraldehyde (with recognized toxic effects), in the design of protein scaffolds for tissue engineering to improve their mechanical properties and to match the degradation rate with the tissue's regeneration one.^[31]

In conclusion, our observations suggest that proteins that do not normally possess characteristics suitable for the production of plasticizing materials can be transformed into innovative materials, leading to the production and accumulation of potential useful next-generation products in the materials and pharmaceutical industry.

AUTHOR CONTRIBUTIONS

Andrea Pompa: Conceptualization; Data curation; Funding acquisition; Project administration; Supervision; Writing – original draft; Writing – review & editing. **Francesca De Marchis:** Data curation; Formal analysis; Investigation; Methodology; Supervision; Validation; Writing – review & editing. **Tania Vanzolini:** Data curation; Formal analysis; Investigation; Methodology; Validation. **Elisa Maricchiolo:** Data curation; Formal analysis; Investigation; Methodology; Validation; Writing – review & editing. **Michele Bellucci:** Conceptualization; Data curation; Formal analysis; Investigation; Methodology; Writing – original draft; Writing – review & editing. **Michele Menotta:** Data curation; Investigation; Methodology; Validation; Writing – original draft. **Tomas Di Mambro:** Data curation; Methodology; Resources; Validation; Visualization. **Annalisa Aluigi:** Data curation; Formal analysis; Investigation; Validation; Writing – review & editing. **Andrea Zattoni:** Data curation; Formal analysis; Investigation; Methodology; Writing – review & editing. **Barbara Roda:** Data curation; Formal analysis; Investigation; Validation. **Valentina Marassi:** Data curation; Formal analysis; Investigation; Validation. **Rita Crinelli:** Data curation; Formal analysis; Funding acquisition; Investigation; Supervision; Validation; Writing – review & editing.

ACKNOWLEDGMENTS

This work has been funded by the European Union – NextGenerationEU under the Italian Ministry of University and Research (MUR) National Innovation Ecosystem grant ECS00000041 – VITALITY–CUPH33C22000430006.

CONFLICT OF INTEREST STATEMENT

The authors declare no conflict of interest.

DATA AVAILABILITY STATEMENT

The data that support the findings of this study are available from the corresponding author upon

ORCID

Michele Bellucci  <https://orcid.org/0000-0001-7476-9603>

Andrea Pompa  <https://orcid.org/0000-0001-9884-5607>

REFERENCES

- Andrady, A. L., & Neal, M. A. (2009). Applications and societal benefits of plastics. *Philosophical Transactions: Biological Sciences*, 364(1526), 1977–1984. <https://doi.org/10.1098/rstb.2008.0304>
- Ryan, P. G., Moore, C. J., van Franeker, J. A., & Moloney, C. L. (2009). Monitoring the abundance of plastic debris in the marine environment. *Philosophical Transactions of the Royal Society B: Biological Sciences*, 364(1526), 1999–2012. <https://doi.org/10.1098/rstb.2008.0207>
- Moslehi, Z., Nafchi, A. M., Moslehi, M., & Jafarzadeh, S. (2021). Aflatoxin, microbial contamination, sensory attributes, and morphological analysis of pistachio nut coated with methylcellulose. *Food Science & Nutrition*, 9(5), 2576–2584. <https://doi.org/10.1002/fsn3.2212>
- Varanko, A., Saha, S., & Chilkoti, A. (2020). Recent trends in protein and peptide-based biomaterials for advanced drug delivery. *Advanced Drug Delivery Reviews*, 156, 133–187. <https://doi.org/10.1016/j.addr.2020.08.008>
- Song, F., & Zhang, L.-M. (2009). Gelation modification of soy protein isolate by a naturally occurring cross-linking agent and its potential biomedical application. *Industrial & Engineering Chemistry Research*, 48(15), 7077–7083. <https://doi.org/10.1021/ie801372f>
- Li, H., Wang, M., Williams, G. R., Wu, J., Sun, X., Lv, Y., & Zhu, L.-M. (2016). Electrospun gelatin nanofibers loaded with vitamins A and E as antibacterial wound dressing materials. *RSC Advances*, 6(55), 50267–50277. <https://doi.org/10.1039/C6RA05092A>
- Sharma, A. K., & Sharma, M. K. (2009). Plants as bioreactors: Recent developments and emerging opportunities. *Biotechnology Advances*, 27(6), 811–832. <https://doi.org/10.1016/J.BIOTECHADV.2009.06.004>
- Lössl, A., Eibl, C., Harloff, H. J., Jung, C., & Koop, H. U. (2003). Polyester synthesis in transplastomic tobacco (*Nicotiana tabacum* L.): Significant contents of polyhydroxybutyrate are associated with growth reduction. *Plant Cell Reports*, 21(9), 891–899. <https://doi.org/10.1007/S00299-003-0610-0>
- Bally, J., Paget, E., Droux, M., Job, C., Job, D., & Dubald, M. (2008). Both the stroma and thylakoid lumen of tobacco chloroplasts are competent for the formation of disulphide bonds in recombinant proteins. *Plant Biotechnology Journal*, 6(1), 46–61. <https://doi.org/10.1111/J.1467-7652.2007.00298.X>
- De Marchis, F., Pompa, A., & Bellucci, M. (2012). Plastid proteostasis and heterologous protein accumulation in transplastomic plants. *Plant Physiology*, 160(2), 571–581. <https://doi.org/10.1104/pp.112.203778>
- Pompa, A., De Marchis, F., Vitale, A., Arcioni, S., & Bellucci, M. (2010). An engineered C-terminal disulfide bond can partially replace the phaseolin vacuolar sorting signal. *The Plant Journal*, 61(5), 782–791. <https://doi.org/10.1111/j.1365-313X.2009.04113.x>
- Marassi, V., De Marchis, F., Roda, B., Bellucci, M., Capecci, A., Reschiglian, P., Pompa, A., & Zattoni, A. (2021). Perspectives on protein biopolymers: Miniaturized flow field-flow fractionation-assisted characterization of a single-cysteine mutated phaseolin expressed in transplastomic tobacco plants. *Journal of Chromatography A*, 1637, 461806. <https://doi.org/10.1016/J.CHROMA.2020.461806>
- De Marchis, F., Pompa, A., Mannucci, R., Morosinotto, T., & Bellucci, M. (2011). A plant secretory signal peptide targets plastome-encoded recombinant proteins to the thylakoid membrane. *Plant Molecular Biology*, 76(3–5), 427–441. <https://doi.org/10.1007/s11103-010-9676-6>
- De Marchis, F., Bellucci, M., & Pompa, A. (2016). Phaseolin expression in tobacco chloroplast reveals an autoregulatory mechanism in heterologous protein translation. *Plant Biotechnology Journal*, 14(2), 603–614. <https://doi.org/10.1111/PBI.12405>
- Freudl, R. (2018). Signal peptides for recombinant protein secretion in bacterial expression systems. *Microbial Cell Factories*, 17(1), 52. <https://doi.org/10.1186/s12934-018-0901-3>
- Pedrazzini, E., Giovinazzo, G., Bielli, A., De Virgilio, M., Frigerio, L., Pesca, M., Faoro, F., Bollini, R., Ceriotti, A., & Vitale, A. (1997). Protein quality control along the route to the plant vacuole. *The Plant Cell*, 9(10), 1869–1880. <https://doi.org/10.1105/TPC.9.10.1869>
- Watson, J., Koya, V., Leppla, S. H., & Daniell, H. (2004). Expression of *Bacillus anthracis* protective antigen in transgenic chloroplasts of tobacco, a non-food/feed crop, a non-food/feed crop. *Vaccine*, 22(31–32), 4374–4384. <https://doi.org/10.1016/j.vaccine.2004.01.069>
- Dhingra, A., Portis Jr, A. R., & Daniell, H. (2004). Enhanced translation of a chloroplast-expressed RbcS gene restores small subunit levels and photosynthesis in nuclear RbcS antisense plants. *Proceedings of the National Academy of Sciences of USA*, 101(16), 6315–6320. <https://doi.org/10.1073/pnas.0400981101>
- Bellucci, M., De Marchis, F., Nicoletti, I., & Arcioni, S. (2007). Zeolin is a recombinant storage protein with different solubility and stability properties according to its localization in the endoplasmic reticulum or in the chloroplast. *Journal of Biotechnology*, 131(2), 97–105. <https://doi.org/10.1016/j.jbiotec.2007.06.004>
- De Marchis, F., Pompa, A., & Bellucci, M. (2016). Chemical secretory pathway modulation in plant protoplasts. *Methods in Molecular Biology*, 1459, 67–79. https://doi.org/10.1007/978-1-4939-3804-9_4
- Marassi, V., Marangon, M., Zattoni, A., Vincenzi, S., Versari, A., Reschiglian, P., Roda, B., & Curioni, A. (2021). Characterization of red wine native colloids by asymmetrical flow field-flow fractionation with online multidetection. *Food Hydrocolloids*, 110, 106204. <https://doi.org/10.1016/j.foodhyd.2020.106204>
- Marassi, V., Giordani, S., Reschiglian, P., Roda, B., & Zattoni, A. (2022). Tracking heme-protein interactions in healthy and pathological human serum in native conditions by miniaturized FFF-multidetector. *Applied Sciences*, 12(13), 6762. <https://doi.org/10.3390/app12136762>
- Frigerio, L., De Virgilio, M., Prada, A., Faoro, F., & Vitale, A. (1998). Sorting of phaseolin to the vacuole is saturable and requires a short C-terminal peptide. *The Plant Cell*, 10(6), 1031–1042. <https://doi.org/10.1105/tpc.10.6.1031>
- Singh, P., Sharma, L., Kulothungan, S. R., Adkar, B. V., Prajapati, R. S., Ali, P. S. S., Krishnan, B., & Varadarajan, R. (2013). Effect of signal peptide on stability and folding of *Escherichia coli* thioredoxin. *PLoS One*, 8(5), e63442. <https://doi.org/10.1371/JOURNAL.PONE.0063442>
- Pilipchuk, S. P., Vaicik, M. K., Larson, J. C., Gazyakan, E., Cheng, M. H., & Brey, E. M. (2013). Influence of crosslinking on the stiffness and degradation of dermis-derived hydrogels. *Journal of Biomedical Materials Research, Part A*, 101(10), 2883–2895. <https://doi.org/10.1002/JBMA.34602>
- Francius, G., Hemmerlé, J., Ohayon, J., Schaaf, P., Voegel, J.-C., Picart, C., & Senger, B. (2006). Effect of crosslinking on the elasticity of polyelectrolyte multilayer films measured by colloidal probe AFM. *Microscopy Research and Technique*, 69(2), 84–92. <https://doi.org/10.1002/jemt.20275>
- Abe, M. M., Martins, J. R., Sanvezzo, P. B., Macedo, J. V., Branciforti, M. C., Halley, P., Botaro, V. R., & Brienzo, M. (2021). Advantages and disadvantages of bioplastics production from starch and lignocellulosic components. *Polymers*, 13(15), 2484. <https://doi.org/10.3390/POLYM13152484>
- Ruf, S., Hermann, M., Berger, I. J., Carrer, H., & Bock, R. (2001). Stable genetic transformation of tomato plastids and expression of a foreign protein in fruit. *Nature Biotechnology*, 19(9), 870–875. <https://doi.org/10.1038/nbt0901-870>
- Oey, M., Lohse, M., Kreikemeyer, B., & Bock, R. (2008). Exhaustion of the chloroplast protein synthesis capacity by massive expression of a highly stable protein antibiotic. *The Plant Journal*, 57(3), 436–445. <https://doi.org/10.1111/j.1365-313X.2008.03702.x>
- Dozier, J., & Distefano, M. (2015). Site-specific PEGylation of therapeutic proteins. *International Journal of Molecular Sciences*, 16(10), 25831–25864. <https://doi.org/10.3390/ijms161025831>

31. Krishnakumar, G. S., Sampath, S., Muthusamy, S., & John, M. A. (2019). Importance of crosslinking strategies in designing smart biomaterials for bone tissue engineering: A systematic review. *Materials Science and Engineering, C*, 96, 941–954. <https://doi.org/10.1016/j.msec.2018.11.081>

SUPPORTING INFORMATION

Additional supporting information can be found online in the Supporting Information section at the end of this article.

How to cite this article: De Marchis, F., Vanzolini, T., Maricchiolo, E., Bellucci, M., Menotta, M., Di Mambro, T., Aluigi, A., Zattoni, A., Roda, B., Marassi, V., Crinelli, R., & Pompa, A. (2023). A biotechnological approach for the production of new protein bioplastics. *Biotechnology Journal*, e2300363. <https://doi.org/10.1002/biot.202300363>